Multi-Omics Integrated Analysis of the Protective Effect of EZH2 Inhibition in Mice with Renal Ischemia-Reperfusion Injury

Shanshan Zou[a] Jianing Chen[a] Peihui Zhou[b] Mengzhu Xue[c] Ming Wu[d]
Li Wang[a]

[a]Department of Nephrology, Shanghai Ninth People's Hospital, Shanghai Jiao Tong University School of Medicine, Shanghai, PR China; [b]Shanghai Diabetes Institute, Department of Endocrinology and Metabolism, Shanghai Sixth People's Hospital Affiliated to Shanghai Jiao Tong University School of Medicine, Shanghai, PR China; [c]Shanghai Jiao Tong University School of Medicine, College of Stomatology, Shanghai Jiao Tong University, National Center for Stomatology, National Clinical Research Center for Oral Diseases, Shanghai Key Laboratory of Stomatology, Shanghai Research Institute of Stomatology, Research Unit of Oral and Maxillofacial Regenerative Medicine, Chinese Academy of Medical Sciences, Shanghai, PR China; [d]Department of Nephrology, Shuguang Hospital Affiliated to Shanghai University of Traditional Chinese Medicine, TCM Institute of Kidney Disease of Shanghai University of Traditional Chinese Medicine, Key Laboratory of Liver and Kidney Diseases, Ministry of Education, Shanghai Key Laboratory of Traditional Chinese Clinical Medicine, Shanghai, PR China

Abstract

Introduction: Acute kidney injury (AKI) is a common clinical syndrome associated with high morbidity and mortality. Inhibition of the methyltransferase enhancer of zeste homolog 2 (EZH2) by its inhibitor 3-deazaneplanocin A (3-DZNeP) exerts renal benefits in acute renal ischemia-reperfusion injury (IRI). However, the underlying mechanisms are not completely known. This study aimed to elucidate the pathological mechanism of EZH2 in renal IRI by combination of multi-omics analysis and expression profiling in a public clinical cohort. ***Methods:*** In this study, C57BL/6 J mice were used to establish the AKI model, which were treated with 3-DZNeP for 24 h. Kidney samples were collected for RNA-seq analysis, which was combined with publicly available EZH2 chromatin immunoprecipitation sequencing (ChIP-seq) data of mouse embryonic stem cell for a joint analysis to identify differentially expressed genes. Several selected differentially expressed genes were verified by quantitative PCR. Finally, single-nucleus sequencing data and expression profiling in public clinical datasets were used to confirm the negative correlation of the selected genes with EZH2 expression. ***Results:*** 3-DZNeP treatment significantly improved renal pathology and function in IRI mice. Through RNA-seq analysis combined with EZH2 ChIP-seq database, 162 differentially expressed genes were found, which might be involved in EZH2-mediated pathology in IRI kidneys. Four differential expressed genes (*Scd1*, *Cidea*, *Ghr*, and *Kl*) related to lipid metabolism or cell growth were selected based on Gene Ontology and Kyoto Encyclopedia of Genes and Genome enrichment analysis, which were validated by quantitative

Shanshan Zou, Jianing Chen, and Peihui Zhou contributed equally to this work.

Correspondence to:
Li Wang, wlyjy73122@126.com
Ming Wu, mingwunl@126.com

Karger

OPEN ACCESS

PCR. Data from single-nucleus RNA sequencing revealed the negative correlation of these four genes with *Ezh2* expression in different subpopulations of proximal tubular cells in IRI mice in a different pattern. Finally, the negative correlation of these four genes with EZH2 expression was confirmed in patients with AKI in two clinical datasets. **Conclusions:** Our study indicates that *Scd1*, *Cidea*, *Ghr*, and *Kl* are downstream genes regulated by EZH2 in AKI. Upregulation of EZH2 in AKI inhibits the expression of these four genes in a different population of proximal tubular cells to minimize normal physiological function and promote acute or chronic cell injuries following AKI.

Introduction

Acute kidney injury (AKI) is a common clinical syndrome characterized by a rapid increase in serum creatinine (Scr) with or without decreased urine output [1]. AKI is associated with high incidence and mortality rates, with a rising trend in hospitalized patients in recent years [2]. There are three recognized causes of AKI, which are prerenal, renal, and postrenal injury. Renal AKI accounts for 80%–90% of cases, which is mainly caused by ischemic injury or nephrotoxins that damage the renal structures [3, 4]. In a clinic, neutrophil gelatinase-associated lipid transport protein (NGAL) and kidney injury molecule 1 (KIM-1) are commonly used diagnostic markers for AKI [5].

Histone modification-mediated epigenetic gene regulation plays an important role in ischemia-reperfusion injury (IRI), which is involved in histone modifications of proinflammatory and profibrotic genes [6]. Polycomb repressive complex 2 (PRC2) is a methyltransferase (HMT) in which the enhancer of zeste homolog 2 (EZH2) is the key subunit that trimethylates lysine 27 on histone H3 (H3K3me27), thereby silencing downstream target gene expression [7]. EZH2 is known to participate in various cellular processes such as cell cycle regulation, DNA damage repair, apoptosis, autophagy, and immunological responses, and thus, EZH2 was extensively studied in various cancers [8–10].

EZH2 and H3K27me3 are upregulated in ischemia-reperfusion (I/R) or folic acid-induced AKI mouse kidneys [11]. The EZH2 inhibitor 3-deazaneplanocin A (3-DZNeP) reduced renal tubular epithelial cell death by preserving cell adhesion/junctions, reducing the expression of matrix metalloproteinases, and attenuating the Raf-2/ERK1/1 pathway in injured kidneys [11]. In another report, inhibition of EZH2 by 3-DZNeP preserved renal function and reduced tubular injury by regulating the p38 signaling pathway and inhibiting cell apoptosis as well as inflammation [12]. It has also been shown that EZH2 can induce the production of reactive oxygen species through the ALK4/Smad5/2 signaling pathway and thus EZH2 inhibition, exerting renal protection by reducing oxidative stress in IRI kidneys [13].

Multi-omics analysis encompasses genomics, transcriptomics, proteomics, and metabolomics [14]. Different omics approaches can be combined to dissect the signaling properties and mechanisms of a disease. For example, chromatin immunoprecipitation sequencing (ChIP-seq) and RNA-seq can be integrated to identify transcriptional regulated genes together with specific genomic DNA binding sites or histone modification [15].

Single-nucleus RNA sequencing (snRNA-seq) is a rapidly evolving technique, which can dissect cellular heterogeneity in complex tissues and characterize rare cell populations at a single-cell resolution [16]. A recent snRNA-seq study on an AKI mouse model revealed two novel clusters of proximal tubular (PT) cells, named NewPT1 and NewPT2, besides the healthy kidney cell clusters PTS1, PTS2, and PTS3 (corresponding to S1, S2, and S3 segments of the PT) [17]. NewPT1 cells belong to a cluster composed of the three acute injury states, while NewPT2 cells belong to a newly identified population of PT cells that fail to repair and expresses abundant proinflammatory and profibrotic genes, suggesting that NewPT2 is a cluster of PT cells that need to be targeted for therapy [17]. In this study, we aimed to investigate the downstream mechanism of EZH2 in renal IRI with integrated multi-omics assays.

Materials and Methods

Animal Models

Wild-type male C57BL/6 J mice aged 6–8 weeks (approx. 22 g) were used to establish the model of AKI induced by I/R. All mice were provided by the animal house of the Central Laboratory of the Ninth Hospital of Shanghai Jiao Tong University. The experimental procedures were approved by the Ethics Committee of the Ninth People's Hospital (SH9H-2020-A655-1). Mice were equally divided into four groups: sham + normal saline (NS), I/R + NS, sham + 3-DZNeP, and I/R + 3-DZNeP. NS or 3-DZNeP (2 mg/kg, Selleck, USA) was intraperitoneally injected at 24 h before surgery. Mice were fasted for 12 h before the surgery. After anesthesia with 2% sodium pentobarbital (40 mg/kg), the abdomen of mouse was exposed, and both renal arteries were clamped for 30 min to achieve kidney ischemia. During this period, the animals were closely monitored to prevent a decrease in body temperature. After the ischemic period, the arterial clamps were removed. If the kidneys changed from dark red to bright red, it indicated a successful modeling. Then, 500 µL of sterile saline was added to the abdominal cavity, and the incision was sutured. The sham mice underwent the same surgical procedure without clamping the renal arteries. At 24 h after reperfusion, the mice were euthanized for blood and kidney collection.
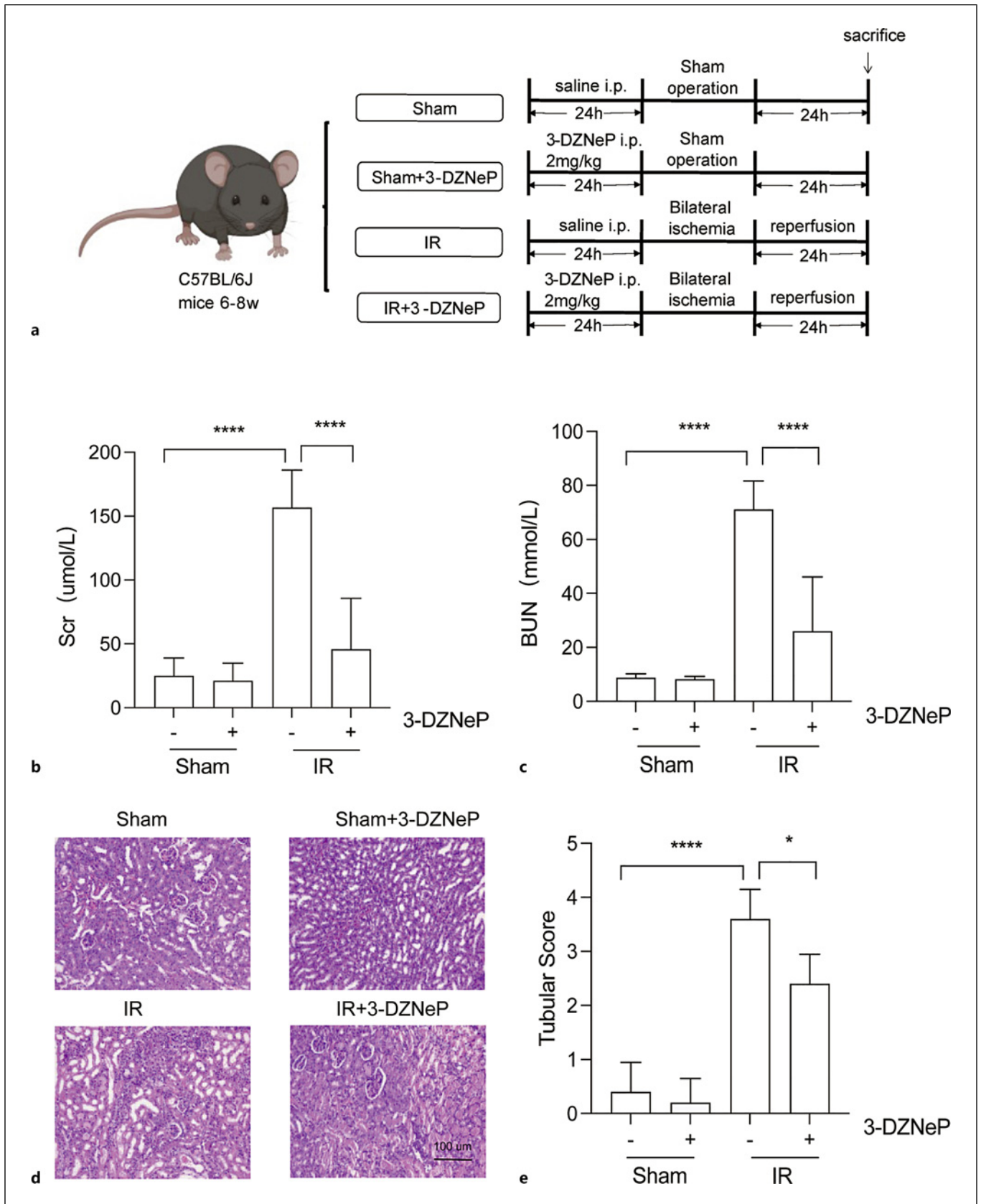
(For legend see next page.)

Zou/Chen/Zhou/Xue/Wu/Wang
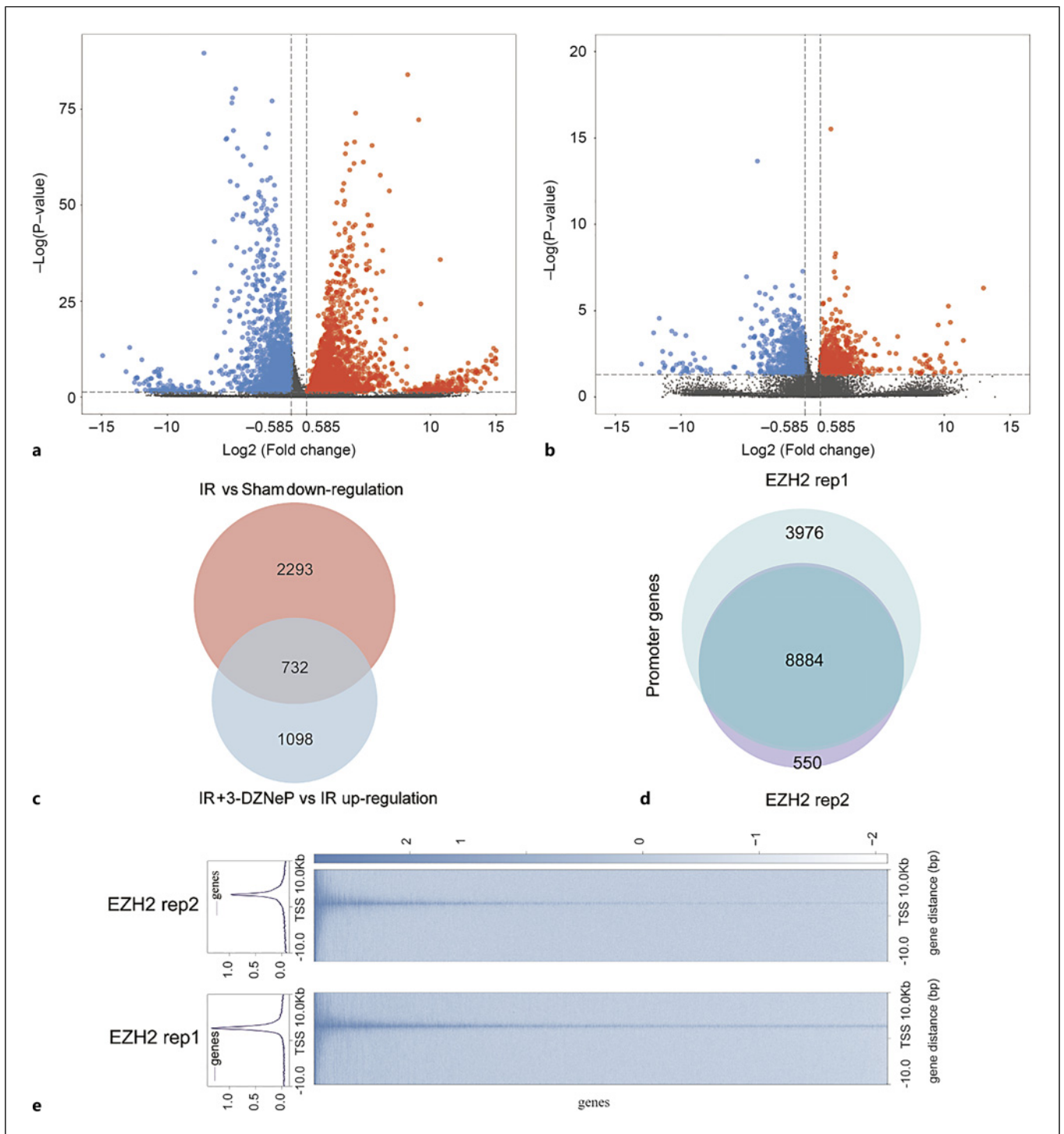
2

(Figure continued on next page.)

Fig. 1. a Inhibition of EZH2 by 3-DZNeP improved IRI in mice. Experimental flowchart (6 mice per group) in male mice upon sham or renal ischemia-reperfusion (I/R) surgery. Serum creatinine (Scr) levels (**b**) and blood urine nitrogen (BUN) levels (**c**) were assessed. **d** HE staining of mouse kidney sections (magnification ×200, bar = 100 μm). **e** Quantitative assessment of tubular injury. NS represents not significant. *$p < 0.05$. **$p < 0.01$. ***$p < 0.001$.
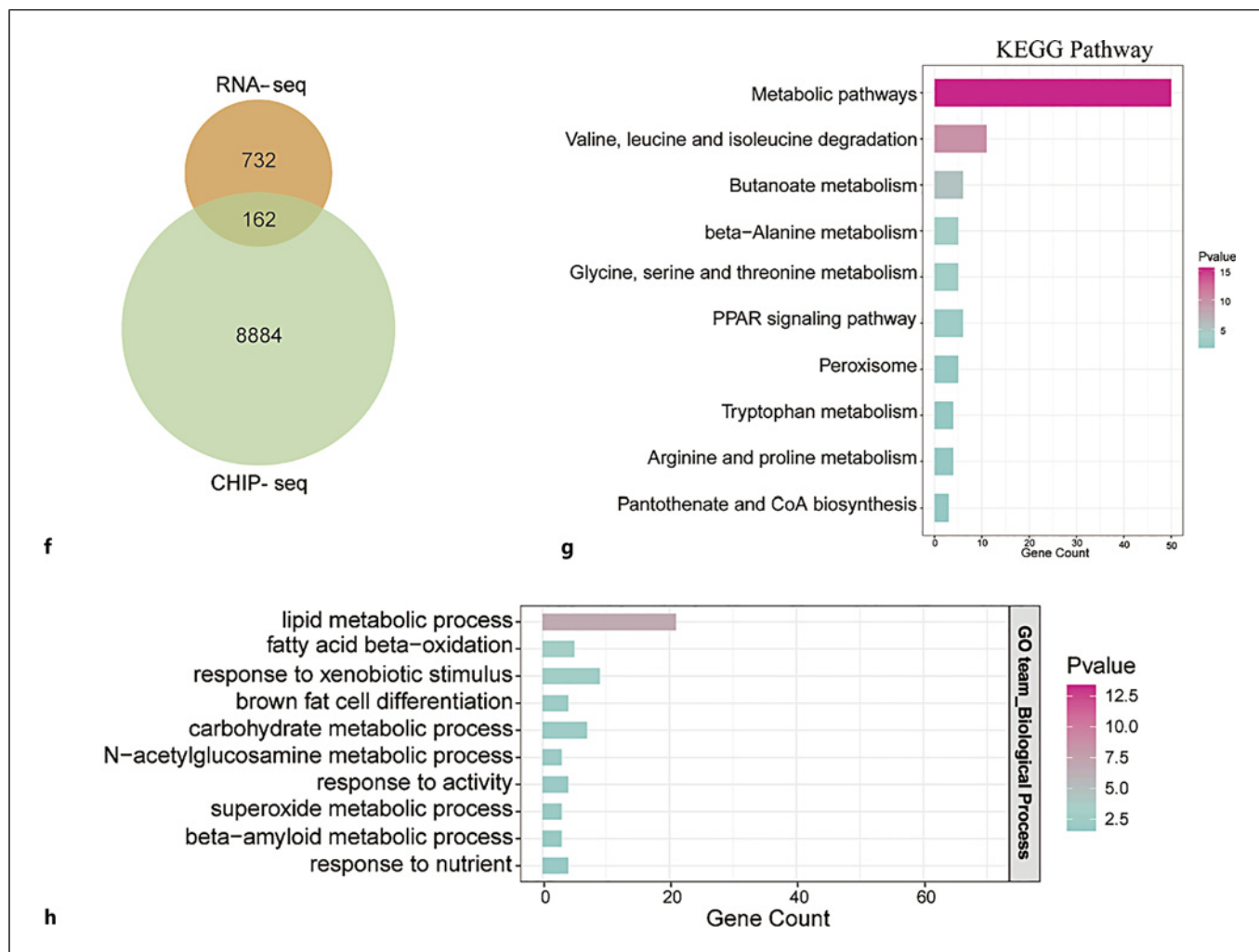
Fig. 2. Combined analysis of RNA-seq and EZH2 ChIP-seq. Three samples per group were collected for RNA-seq analysis from mice upon sham or IR operation with or without 3-DZNep treatment. **a** Volcano plot of differentially expressed genes between ischemia-reperfusion (IR) versus sham group. **b** Volcano plot of differentially expressed genes between IR + 3-DZNeP versus IR group. **c** Venn diagram of genes from RNA-seq data. **d** Venn diagram of genes from the two biological replicates of EZH2 ChIP-seq. **e** ChIP-seq signal profiles and binding peak heatmap. **f** Venn diagram of RNA-seq and EZH2 ChIP-seq data. **g** Kyoto Encyclopedia of Genes and Genomes (KEGG) analysis of 162 differential genes. **h** Gene Ontology (GO) analysis of 162 differential genes. Promoter region (including ≤1 kb, 1–2 kb, and 2–3 kb). "*p* value" refers to the statistical significance level. TSS, transcription start site; rep1-rep2, biological replicates.

Renal Function Measurements

The blood collected from the eyeball was centrifuged at 3,000× for 15 min, and the supernatant was sent to the Department of Laboratory of the Ninth People's Hospital for enzymatic analysis of Scr and blood urea nitrogen.

RNA Extraction and Real-Time Fluorescence Quantitative PCR

Total RNA was extracted from kidney tissue using TRIzol reagent (15596-026, Thermo Fisher Scientific, USA) and then reverse-transcribed to generate cDNA using a Takara kit (Takara Bio, Shiga, Japan). The cDNA was subsequently subjected to qPCR amplification using SYBR Green premix

(Yeasen, Shanghai, China) following standard methods. The relative gene expression was normalized to GAPDH. The primer sequences are listed in Table 1.

HE Staining

Kidney tissues were fixed by 10% paraformaldehyde. After embedding in paraffin, the specimens were sectioned and subjected to deparaffinization, dehydration, and staining with hematoxylin and eosin. Histological evaluation of kidney injury was performed under a light microscope.

All histological examinations were conducted by pathologists in a blinded manner. Renal pathological abnormalities were scored based on the presence and severity of components such as tubular

Zou/Chen/Zhou/Xue/Wu/Wang

Table 1. Sequences of real-time PCR primers

Gene name	Primer sequence (5′ → 3′)	Primer sequence (3′ → 5′)
Mouse NGAL	ACCACGGACTACAACCAGTTCG	ACTTGGCAAAGCGGGTGAAAC
Mouse Kim-1	CTGCTGCTACTGCTCCTTGTG	CACGCTTAGAGATGCTGACTTCC
Mouse Scd1	GCCTGTTCGTTAGCACCTTCTTG	GGGATTGAATGTTCTTGTCGTAGGG
Mouse Cidea	CCGTGTTAAGGAATCTGCTGAGG	GGATGGCTGCTCTTCTGTATCG
Mouse Ghr	GTACAGCGAGTTCAGCGAAGTC	GGTGATACAGGTGGTTGTCAATCTC
Mouse GAPDH	AGGTCGGTGTGAACGGATTTG	TGTAGACCATGTAGTTGAGGTCA
Mouse Ezh2	AGAGTGGAAGCAGCGGAGGATAC	CATTATAGGCACCGAGGCGACTG
Mouse Kl	TGACTTTGTGCTAGGCTGGTTTG	AATCAGGCAGAAGAGACGAGAGG

Table 2. Differentially expressed genes screened by RNA-seq and CHIP-seq

Gene	log2FC (IR/sham)	log2FC (IR + 3-DZNeP/IR)	Description
Cidea	−5.235	3.860	Lipid transferase Cidea
Scd1	−4.729	2.928	Acyl-CoA desaturase 1
Ghr	−2.677	0.657	Growth hormone receptor
Kl	−2.128	1.010	Klotho
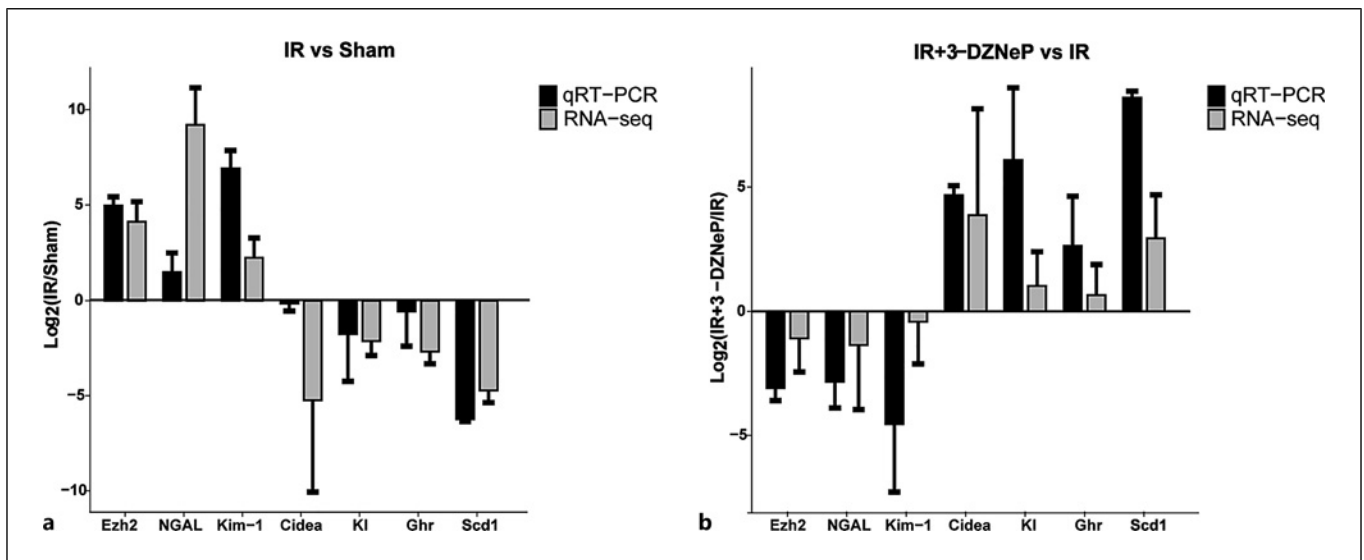
Fig. 3. PCR validation of EZH2-targeted genes. Quantitative PCR validation was performed and compared with RNA-seq data. **a** Results of differential expressed genes between the IR versus sham group were validated by quantitative PCR. **b** Results of differential expressed genes between the IR + 3-DZNeP versus IR group was validated.

necrosis or injury, loss of the brush border, tubular dilation, cell lysis, and tubular cast formation: 0 = normal kidney (no injury); 1 = minimal injury (<25% injury); 2 = mild injury (25–50% injury); 3 = moderate injury (50–75% injury); 4 = severe injury (>75% injury).

RNA Sequencing Determination and Data Analysis

Total mRNA was isolated from mouse kidney tissues ($n = 3$) by TRIzol (B511311, Sangon Biotech, China). mRNA libraries were prepared with the Hieff NGS™ MaxUp Dual-mode mRNA Library Prep Kit from Illumina® (12301ES96,YEASEN, China)
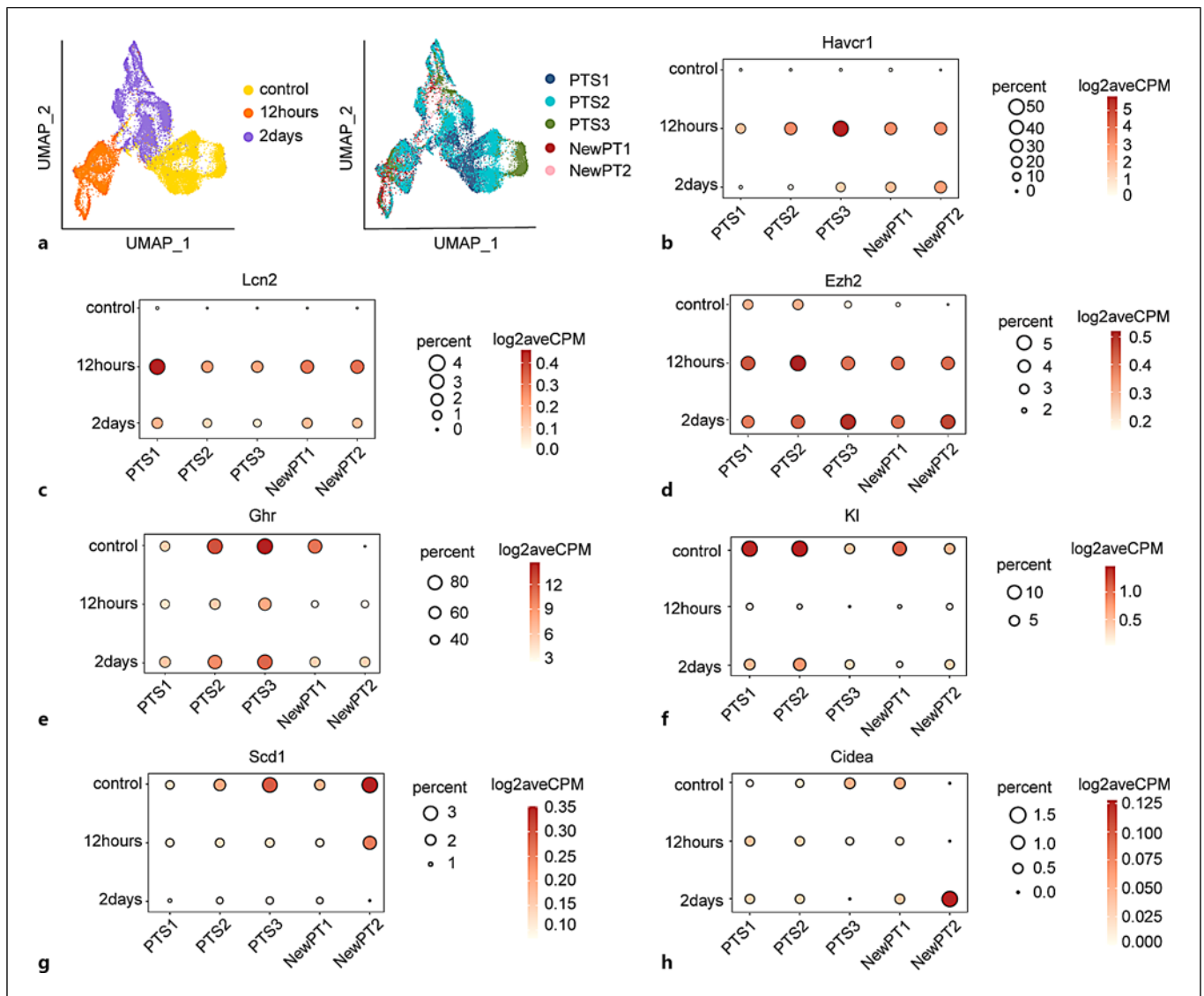
Fig. 4. Analysis of four selected EZH2 downstream genes by snRNA-seq. The snRNA-seq samples were collected from 8- to 10-week-old male mice. Ischemia was induced by clamping of the bilateral renal pedicles for 18 min. Mice were sacrificed at 4 and 12 h and 2, 14, and 42 days post bilateral ischemia-reperfusion injury (IRI). In this study, UMI count data from the control, 12-h, and 2-day samples were reanalyzed. **a** UMAP plot displays clustering of all PT cells. **b** Bubble plot depicting the proportion of positive cells for the *Havcr1* gene. **c** Bubble plot depicting the proportion of positive cells for the *Lcn2* gene. **d** Bubble plot depicting the proportion of positive cells for the *Ezh2* gene. **e** Bubble plot depicting the proportion of positive cells for the *Ghr* gene.

f Bubble plot depicting the proportion of positive cells for the *Kl* gene. **g** Bubble plot depicting the proportion of positive cells for the *Scd1* gene. **h** Bubble plot depicting the proportion of positive cells for the *Cidea* gene. PT-S1 represents the S1 segment of the PT; PT-S2 corresponds to the S2 segment of the PT; PT-S3 corresponds to the S3 segment of the PT. "NewPT1" and "NewPT2" are newly identified clusters that emerge during injury, located proximate to healthy PTs in the UMAP space, representing the injury state of mouse PTs. "Log2 average counts per million (log2avecpm)" is a metric computed from sequencing data to represent the expression levels of each gene or transcript at the single-cell level.

following the manufacturer's instructions. Quality control was performed using gel electrophoresis. Subsequently, libraries were sequenced in PE150 mode on Illumina Hiseq™ instruments at Sangon Biotech (Shanghai, China).

Reads were aligned to the mm10 mouse genome for read count and transcript per million data generation. Differential gene expression analysis was performed using edgeR (v3.36.0) in R 4.2.0. Differentially expressed genes were identified based
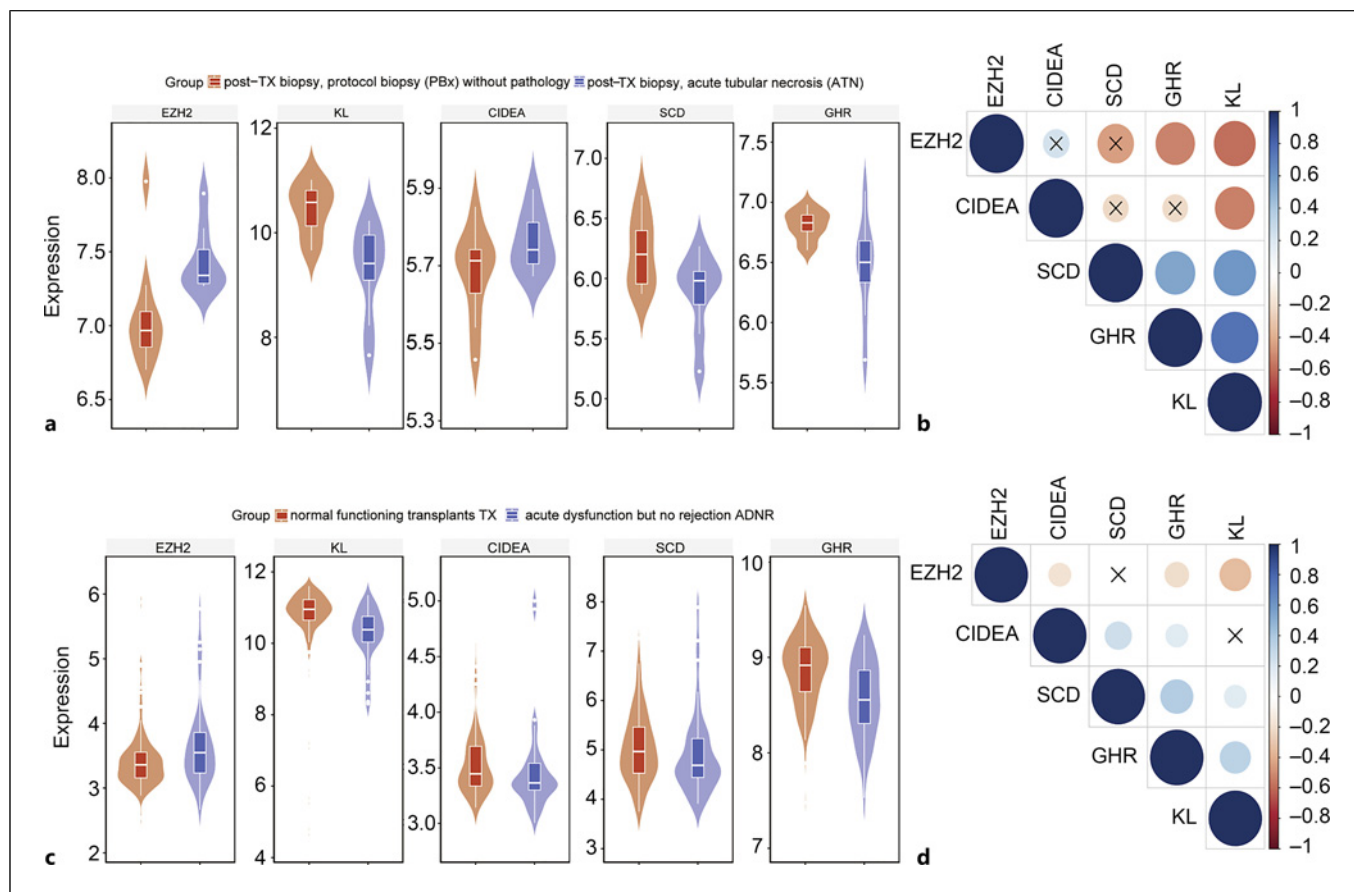
Fig. 5. Violin plots of EZH2 regulated gene expression in public clinical datasets. **a** GSE 53769 comprises 8 posttransplant (Tx) biopsy with acute tubular necrosis (ATN) and 10 post-Tx biopsy with protocol biopsy (PBx) without pathology. Violin plots of key gene expression in the GSE53769 database. **b** Pearson correlation between the EZH2 gene and the four selected genes in the GSE 53769 dataset. The GSE 76882 dataset consists of 99 normal functioning transplant samples and 40 samples with acute dysfunction but no rejection. **c** Violin plots of key gene expression in the GSE76882 database. **d** Pearson correlation between the EZH2 gene and the four selected genes in the GSE76882 dataset.

on the criteria: *p* value <0.05 and absolute FC ≥1.5 (equivalent to |log2FC| ≥ 0.585). GO enrichment analysis and KEGG pathway analysis were performed using the DAVID database (https://david.ncifcrf.gov/). GO functional analysis included biological processes, molecular functions, and cellular components. Statistical significance was determined with adjusted *p* values using the Benjamini and Hochberg method, where corrected *p* value <0.05 indicated significance for differential expression.

Public ChIP-Seq Data Acquirement and Analysis

EZH2 ChIP-seq data from mouse embryonic stem cells were obtained from NCBI-GEO using SRA software suite (version 3.0.0). The dataset included input samples (GSM1199187) and two EZH2 antibody-treated biological replicates (GSM1199182 and GSM1199183) [18]. After aligning to the mm10 genome with bowtie2 software (version 2.0.5), peak calling was performed using the HOMER software suite (version 4.11.1). File formats were converted using Samtools software (version 1.1), and peak annotation was conducted with ChIPseeker software (version 1.32.1).

Single-Cell Transcriptome Sequencing Acquirement and Analysis

Download metadata for the single-cell nuclear transcriptome sequencing dataset GSE139107 from the GEO website, including UMI count data for control, 12 h, and 2 days samples after IRI. The UMI count data related to PTS1, PTS2, PTS3, NewPT1 (new PT subpopulation 1), and NewPT2 (new PT subpopulation 2) were extracted based on cell type annotation using Seurat (v4.3.0.1) in R 4.2.0 [17]. The data were transformed into log2 count per million +1 values to depict expression levels. After data standardization, feature search, principal component analysis, and clustering, UMAP clusters were separately visualized based on sample time points and sources. Then, we extracted the cell expression matrix of key genes and calculated the single-cell

average expression level of genes and the proportion of cells with an expression level ≥1. Finally, positive percentage bubbles were plotted in R 4.2.0.

Expression Profiling Validation in Public Datasets

GSE227970, GSE53769, and GSE76882 datasets were obtained from the GEO database (http://www.ncbi.nlm.nih.gov/geo/). Candidate gene expressions across different groups were extracted and visualized in R 4.2.0. Pearson correlation coefficients were calculated for correlation analysis, with a significance level set at $p < 0.05$, indicating significant correlations between the genes.

Statistical Analysis

Data were presented as mean ± standard deviation. Two-group comparisons were performed using t-tests, while comparisons among multiple groups were conducted using ANOVA. GraphPad Prism software was used for data analysis, and R package ggplot2 (v3.4.2) was used for data visualization. p value <0.05 was considered statistically significant.

Results

Inhibition of EZH2 by 3-DZNeP Preserved Renal Function and Attenuated Tubular Injury in IRI Mice

IRI was performed by bilateral renal artery clamping for 30 min and followed by 24 h of reperfusion in C57 mice (Fig. 1a). Scr and blood urea nitrogen levels were significantly higher in the IRI group compared to the sham group, which were reduced by 24 h pretreatment with 2 mg/kg 3-DZNeP (Fig. 1b, c). HE staining revealed that renal histology was injured in IRI kidneys, as shown by reduced tubular epithelial cell swelling, tubular dilation, and less tubular cell nuclear dissolution, which was improved by 3-DZNeP treatment (Fig. 1d). Renal injury was further quantified and showed that 3-DZNeP treatment significantly reduced the score of tubular injury in IRI kidneys (Fig. 1e). These results indicate that inhibition of EZH2 by 3-DZNeP prevents renal injury in IRI mice.

Analysis of Differentially Expressed Genes Regulated by EZH2

A total of 7,026 differential genes were identified between the IR (I/R) group and the sham group (with p value <0.05, fold change [FC] absolute value ≥1.5). Among these, 4,733 genes were upregulated in the IR mice, while 2,293 genes were downregulated (Fig. 2a). There were 2,361 differential genes between the IR + 3-DZNeP group and the IR group (p value <0.05, FC absolute value ≥1.5), of which 1,098 genes were upregulated in expression and 1,263 genes were downregulated in the IR mice (Fig. 2b).

Given that EZH2 is an epigenetic regulator of gene silencing and EZH2 is upregulated in AKI, we further selected differentially expressed genes that were downregulated in the IRI group and upregulated in the treatment group for subsequent study. A total of 732 differentially expressed genes were identified (Fig. 2c).

We next downloaded a public dataset for EZH2 ChIP-seq analysis of mouse embryonic stem cells (GSE49431) to search the direct targeted genes of EZH2. The ChIP-seq signal profiles were derived from the two biological replicates, which showed strong high enrichment of binding peaks near the transcription start site (Fig. 2e). A total of 8,884 genes with EZH2 enrichment in the promoter region were obtained from two biological replicates (Fig. 2d).

A joint analysis of RNA-seq and EZH2 ChIP-seq data was further performed. And the final 162 differentially expressed genes with EZH2 enrichment in their promoter region were obtained (Fig. 2f). Kyoto Encyclopedia of Genes and Genome (KEGG) pathway enrichment analysis and Gene Ontology (GO) functional enrichment analysis were performed. The 162 differentially expressed genes were mainly associated with the metabolic pathways, which were revealed by KEGG analysis (Fig. 2g). GO analysis showed that the differentially expressed genes are primarily involved in lipid metabolism as shown in Figure 2h.

Expression of EZH2-Targeted Genes in IR Mouse Kidneys

We selected four genes, *Scd1*, *Cidea*, *Ghr*, and *Kl*, for further validation because these genes are involved in lipid metabolism or cell growth, which is another key feature of AKI (Table 2). Quantitative PCR was performed to validate these differential expressed genes, which were compared with RNA-seq data (Fig. 3a, b). The analysis showed that the mRNA levels of these four genes were significantly decreased in IRI kidneys ($p < 0.05$), with a significantly increased after 3-DZNeP treatment ($p < 0.01$) (Fig. 3a, b). Furthermore, we demonstrated that the expression of these four genes were negatively correlated with the expression of *Ezh2* and two injury markers (*Kim-1* and *NGAL*) in IRI kidneys or 3-DZNeP-treated IRI kidneys (Fig. 3a, b).

Interestingly, we confirmed the negative correlation of EZH2 with KL, SCD1, and GHR expression in a cellular model of cisplatin-induced AKI. In the GSE227970 dataset, the expression of the EZH2 gene increased in the cisplatin-induced AKI group compared to the control group (online suppl. Fig. S1; for all online suppl. material,

see https://doi.org/10.1159/000537866). Moreover, the expression of KL, SCD1, and GHR significantly decreased in the AKI group (online suppl. Fig. S1). Importantly, there was a clear negative correlation between these genes and EZH2 (online suppl. Fig. S1). The expression of the Cidea gene was consistently recorded as zero (data not shown), likely due to the limitation of sequencing technology. Thus, we excluded this gene during quality control.

Expression of EZH2-Targeted Genes in Renal PTs

According to previous studies, the PTs experience the most significant damage due to their high metabolic activity during IRI [17]. Therefore, we selected an snRNA-seq dataset with a similar experimental design to analyze the expression profiles of these four genes in various subpopulations of PT cells (GSE139107). Renal samples were taken at different time points (control, 12 h, and 2 days) after reperfusion, and PT cells were clustered into different groups according to their segment markers (PTS1, PTS2, and PTS3) or injury markers (NewPT1 and NewPT2) (Fig. 4a).

We first analyzed the expression of two injury markers *Lcn2* (NGAL) and *Havcr1* (Kim-1), which were quickly upregulated and reach a peak at 12 h after reperfusion in all five subgroups (Fig. 4b, c). *Ezh2* was upregulated after reperfusion in all five subgroups but only reached a peak at 12 h after reperfusion in PTS1 and PTS2. In PTS3, NewPT1, and NewPT2 cells, *Ezh2* was persistently upregulated at 12 h and 24 h after reperfusion (Fig. 4d).

An acute response of gene downregulation in PTS1 and PTS2 cells was only observed for *Ghr* and *Kl* genes, which was negatively and tightly correlated with *Ezh2* gene expression (Fig. 4e, f). A steadily reduced gene expression in PTS3, NewPT1, and NewPT2 cells was observed for *Scd1* (Fig. 4g). The Cidea gene was only negatively and tightly correlated with *Ezh2* expression in PTS3 cells after reperfusion (Fig. 4h). These results indicate that these four genes are differentially regulated by EZH2 in different subgroups of PT, which may contribute to the acute or chronic responses after renal injury.

Expression of EZH2-Targeted Genes in Patients with Kidney Injury

We next determined the correlation of these four genes with EZH2 in patients with AKI by analyzing the expression profiles of two highly annotated public clinical cohorts (GSE 53769 and GSE 76882), which were downloaded from the GEO website. The violin plots were generated based on the expression profiles from the GSE53769 dataset. The expression of the EZH2 gene was notably increased in the ATN group compared to the PBx group, while the expression of KL, SCD1, and GHR genes were decreased (Fig. 5a). KL and GHR exhibited a strong and negative correlation with EZH2 expression in this dataset, while SCD1 was weakly and negatively correlated with EZH2 expression in this dataset (Fig. 5b).

A similar result was obtained from the GSE76882 dataset. The upregulation of EZH2 and downregulation of KL, SCD1, GHR, and Cidea genes were observed in patients with acute kidney injuries (Fig. 5c). Interestingly, in this dataset, we only observed a negative correlation of EZH2 expression with KL, GHR, and Cidea genes (Fig. 5d).

Discussion

In the current study, we first identified 162 EZH2 regulated genes in the kidneys of AKI mouse through RNA-seq analysis, which was combined with the ChIP-seq analysis. We further selected and verified four genes (*Scd1*, *Cidea*, *Ghr*, and *Kl*) involved in lipid metabolism or cell growth after KEGG and GO enrichment analysis of these 162 genes. By leveraging single-nucleus RNA-seq datasets, we confirmed the negative correlation of these four genes with EZH2 in the PT of AKI kidneys. The negative correlation of these four genes with EZH2 was finally confirmed in patients with acute kidney injuries.

The *Scd1* gene plays a crucial role in lipid metabolism by primarily participating in the intracellular triglyceride synthesis [19]. It has been reported that the EZH2 inhibitor increased the expression of SCD1 in cancer cells [20]. *Cidea* is another gene playing an important role in lipid metabolism, which was found negatively regulated by EZH2 in our study [21]. It has been shown that lipid metabolism gradually declines with prolonged reperfusion time, leading to a higher risk of kidney fibrosis [17]. Our study implies that EZH2 may inhibit lipid metabolism through downregulation of SCD1 and Cidea. Interestingly, in PTS3, NewPT1, and NewPT2 cells, a steadily reduced gene expression of *Scd1* was observed at 12 h and 24 h after reperfusion, which was tightly and negatively correlated with *Ezh2* expression. A negative correlation between *Cidea* and *Ezh2* expression was observed in PTS3 cells. Thus, EZH2 may inhibit lipid metabolism of a different population of PT cells contributing to normal physiological function, acute responses, and chronic responses of PTs after IRI-AKI.

The *Kl* and *Ghr* genes are involved in cell growth and apoptosis [22–25]. During AKI, the expression of the *Kl*

gene in renal tubular cells is reduced, and its restoration can alleviate kidney damage and promote AKI recovery [26, 27]. A significant decrease in GHR expression was observed in diabetic kidney disease, and GHR antagonists protected against diabetic kidney disease [28, 29]. Interestingly, we observed an acute downregulation of *Kl* and *Ghr* in PTS1 and PTS2 cells, which was negatively correlated with *Ezh2* expression. Thus, EZH2 may inhibit cell growth in PTS1 and PTS2 to maintain a minimized physiological function of PTs after IRI-AKI.

The IRI-AKI model is the focus of this study. In order to confirm that our discovered molecular mechanisms can be shared by other type of AKI, we performed analysis on a publicly available RNA-seq data from a cisplatin-AKI model. We found that the expression of KL, SCD1, and GHR were significantly decreased in the cisplatin-AKI group, which was negatively correlated with EZH2 expression.

EZH2 dysregulation is associated with various tumorigenesis and cancer types. Hypermethylation, considered an early event in renal cell carcinoma (RCC), correlates with tumor invasiveness [30]. Inhibiting EZH2 can reactivate PEG3, thereby inhibiting RCC progression [31]. Surgery is the primary treatment for RCC, and nephron-sparing surgery (NSS) is the preferred option to minimize peripheral lesions [30]. During NSS, interruption of renal blood flow may induce kidney injury, representing a distinct pathological cause leading to IRI [32]. Thus, we speculate that our results may have potential applications particularly to IRI-AKI induced by NSS during RCC treatment, in which inhibition of EZH2 may not only inhibit residual RCC after surgery but also prove beneficial to the injured kidney.

One limitation in our study is that we validate these genes only at mRNA levels. The existing literature suggests direct regulation of the *Scd1* gene by EZH2 in mRNA and protein levels in cancer cells [20]. However, direct evidence of *Scd1* regulation by EZH2 in AKI-related studies is currently lacking. Epigenetic regulation of the *Cidea* gene has been shown in a study on intrauterine malnutrition, but direct evidence of Cidea protein regulation by histone modification is lacking [33]. The Ghr gene's epigenetic regulation has not been reported. Interestingly, H3K27me3-mediated epigenetic regulation of the *Kl* gene has been studied in renal tubular cells, and inhibition of H3K27 methylation resulted in elevated Klotho expression [34]. Thus, we propose that proteins encoded by the *Kl* gene may participate in this epigenetic cascade and represent promising candidates as downstream targets for further studies.

In both human and animal models of AKI, consistent downregulation of Klotho is observed [26, 35]. Importantly, mice subjected to IRI exhibit reduced Klotho levels in the kidneys, urine, and blood, preceding the increase in NGAL, indicating an early response [26]. More importantly, ELISA kits and immunoprecipitation-immunoblot kits for detecting Klotho are commercially available [36]. Thus, the activation of the EZH2 signaling pathway after AKI can be indirectly detected through analyzing Klotho expression. EZH2 inhibitors are currently undergoing clinical trials for cancer patients. Tazemetostat, an orally administered selective EZH2 inhibitor, displays anti-tumor activity in both hematological malignancies and solid tumors [37]. As the pioneer among selective EZH2 inhibitors, tazemetostat underwent its initial human studies in 2018, revealing promising safety and anti-tumor efficacy in blood and solid cancer patients [38]. In 2020, tazemetostat entered phase 2 trials for patients with relapsed or refractory follicular lymphoma, which exhibited clinical significance and enduring responses, and maintained favorable tolerability [39]. Once available in the market, EZH2 inhibitors could be applied to AKI patients, particularly RCC patients undergoing NSS, where detection of EZH2 activation becomes important.

In conclusion, our study indicates that *Scd1*, *Cidea*, *Ghr*, and *Kl* are downstream genes regulated by EZH2 in IRI-AKI. Upregulation of EZH2 in IRI-AKI inhibits the expression of these four genes in a different population of PTs to minimize normal physiological function and to promote acute or chronic cell injuries following IRI-induced AKI. Understanding the working mechanism of EZH2 in AKI may help to design a therapy specifically targeting a certain subpopulation of PT to improve repairing and reduce fibrosis after IRI-AKI.

Statement of Ethics

All animal experiments were in accordance with Institutional Animal Care and Use Committee guidelines. This study protocol was reviewed and approved by the Ethics Committee of the Ninth People's Hospital, approval number SH9H-2020-A655-1.

Conflict of Interest Statement

The authors have no conflicts of interest to declare.

Funding Sources

Author Contributions

L.W. and M.W. conceived and designed the study; S.Z., J.C., and M.X. performed the research; S.Z., P.Z., and M.X. analyzed the data; S.Z. and M.W. wrote the paper.

Data Availability Statement

All data generated or analyzed during this study are included in this article. Further inquiries can be directed to the corresponding author.

References

1 Ronco C, Bellomo R, Kellum JA. Acute kidney injury. Lancet. 2019;394(10212):1949–64.

2 Negi S, Koreeda D, Kobayashi S, Yano T, Tatsuta K, Mima T, et al. Acute kidney injury: epidemiology, outcomes, complications, and therapeutic strategies. Semin Dial. 2018;31(5):519–27.

3 Farrar A. Acute kidney injury. Nurs Clin North Am. 2018;53(4):499–510.

4 Basile DP, Anderson MD, Sutton TA. Pathophysiology of acute kidney injury. Compr Physiol. 2012;2:1303–53.

5 Kashani K, Cheungpasitporn W, Ronco C. Biomarkers of acute kidney injury: the pathway from discovery to clinical adoption. Clin Chem Lab Med. 2017;55(8):1074–89.

6 Zager RA, Johnson AC. Renal ischemia-reperfusion injury upregulates histone-modifying enzyme systems and alters histone expression at proinflammatory/profibrotic genes. Am J Physiol Renal Physiol. 2009;296(5):F1032–41.

7 Duan R, Du W, Guo W. Ezh2: a novel target for cancer treatment. J Hematol Oncol. 2020; 13(1):104.

8 Liu Y, Yang Q. The roles of ezh2 in cancer and its inhibitors. Med Oncol. 2023;40(6):167.

9 Holm K, Grabau D, Lovgren K, Aradottir S, Gruvberger-Saal S, Howlin J, et al. Global h3k27 trimethylation and ezh2 abundance in breast tumor subtypes. Mol Oncol. 2012;6(5):494–506.

10 Hu J, Zheng Z, Lei J, Cao Y, Li Q, Zheng Z, et al. Targeting the ezh2-ppar axis is a potential therapeutic pathway for pancreatic cancer. PPAR Res. 2021;2021:5589342.

11 Zhou X, Zang X, Guan Y, Tolbert T, Zhao TC, Bayliss G, et al. Targeting enhancer of zeste homolog 2 protects against acute kidney injury. Cell Death Dis. 2018;9(11):1067.

12 Liang H, Huang Q, Liao MJ, Xu F, Zhang T, He J, et al. Ezh2 plays a crucial role in ischemia/reperfusion-induced acute kidney injury by regulating p38 signaling. Inflamm Res. 2019;68(4):325–36.

13 Liu H, Chen Z, Weng X, Chen H, Du Y, Diao C, et al. Enhancer of zeste homolog 2 modulates oxidative stress-mediated pyroptosis in vitro and in a mouse kidney ischemia-reperfusion injury model. FASEB J. 2020;34(1):835–52.

14 Olivier M, Asmis R, Hawkins GA, Howard TD, Cox LA. The need for multi-omics biomarker signatures in precision medicine. Int J Mol Sci. 2019;20(19):4781.

15 Mimura I, Kanki Y, Kodama T, Nangaku M. Revolution of nephrology research by deep sequencing: chip-seq and rna-seq. Kidney Int. 2014;85(1):31–8.

16 Schreibing F, Kramann R. Mapping the human kidney using single-cell genomics. Nat Rev Nephrol. 2022;18(6):347–60.

17 Kirita Y, Wu H, Uchimura K, Wilson PC, Humphreys BD. Cell profiling of mouse acute kidney injury reveals conserved cellular responses to injury. Proc Natl Acad Sci U S A. 2020;117(27):15874–83.

18 Kaneko S, Son J, Shen SS, Reinberg D, Bonasio R. Prc2 binds active promoters and contacts nascent rnas in embryonic stem cells. Nat Struct Mol Biol. 2013;20(11):1258–64.

19 Nakamura MT, Yudell BE, Loor JJ. Regulation of energy metabolism by long-chain fatty acids. Prog Lipid Res. 2014;53:124–44.

20 Zhang T, Guo Z, Huo X, Gong Y, Li C, Huang J, et al. Dysregulated lipid metabolism blunts the sensitivity of cancer cells to ezh2 inhibitor. EBioMedicine. 2022;77:103872.

21 Puri V, Ranjit S, Konda S, Nicoloro SM, Straubhaar J, Chawla A, et al. Cidea is associated with lipid droplets and insulin sensitivity in humans. Proc Natl Acad Sci U S A. 2008;105(22):7833–8.

22 Neyra JA, Hu MC, Moe OW. Klotho in clinical nephrology: diagnostic and therapeutic implications. Clin J Am Soc Nephrol. 2020;16(1):162–76.

23 Stiedl P, McMahon R, Blaas L, Stanek V, Svinka J, Grabner B, et al. Growth hormone resistance exacerbates cholestasis-induced murine liver fibrosis. Hepatology. 2015;61(2):613–26.

24 Chen K, Wang S, Sun QW, Zhang B, Ullah M, Sun Z. Klotho deficiency causes heart aging via impairing the nrf2-gr pathway. Circ Res. 2021;128(4):492–507.

25 Yan HZ, Wang HF, Yin Y, Zou J, Xiao F, Yi LN, et al. Ghr is involved in gastric cell growth and apoptosis via pi3k/akt signalling. J Cell Mol Med. 2021;25(5):2450–8.

26 Hu MC, Shi M, Zhang J, Quinones H, Kuro-o M, Moe OW. Klotho deficiency is an early biomarker of renal ischemia-reperfusion injury and its replacement is protective. Kidney Int. 2010;78(12):1240–51.

27 Valino-Rivas L, Cuarental L, Ceballos MI, Pintor-Chocano A, Perez-Gomez MV, Sanz AB, et al. Growth differentiation factor-15 preserves klotho expression in acute kidney injury and kidney fibrosis. Kidney Int. 2022; 101(6):1200–15.

28 Chen S, Li B, Chen L, Jiang H. Identification and validation of immune-related biomarkers and potential regulators and therapeutic targets for diabetic kidney disease. BMC Med Genomics. 2023;16(1):90.

29 Oh Y. The insulin-like growth factor system in chronic kidney disease: pathophysiology and therapeutic opportunities. Kidney Res Clin Pract. 2012;31(1):26–37.

30 Minardi D, Lucarini G, Filosa A, Milanese G, Zizzi A, Primio RD, et al. Prognostic role of global dna-methylation and histone acetylation in pt1a clear cell renal carcinoma in partial nephrectomy specimens. J Cell Mol Med. 2009;13(8B):2115–21.

31 Qiu T, Ding Y, Qin J, Ren D, Xie M, Qian Q, et al. Epigenetic reactivation of peg3 by ezh2 inhibitors suppresses renal clear cell carcinoma progress. Cell Signal. 2023;107:110662.

32 Lahoud Y, Hussein O, Shalabi A, Nativ O, Awad H, Khamaisi M, et al. Effects of phosphodiesterase-5 inhibitor on ischemic kidney injury during nephron sparing surgery: quantitative assessment by ngal and kim-1. World J Urol. 2015;33(12):2053–62.

33 Urmi JF, Itoh H, Muramatsu-Kato K, Kohmura-Kobayashi Y, Hariya N, Jain D, et al. Plasticity of histone modifications around cidea and cidec genes with secondary bile in the amelioration of developmentally-programmed hepatic steatosis. Sci Rep. 2019;9(1):17100.

34 Han X, Sun Z. Epigenetic regulation of KL (klotho) via H3K27me3 (histone 3 lysine [K] 27 trimethylation) in renal tubule cells. Hypertension. 2020;75(5):1233–41.

35 Qian Y, Che L, Yan Y, Lu R, Zhu M, Xue S, et al. Urine klotho is a potential early biomarker for acute kidney injury and associated with poor renal outcome after cardiac surgery. BMC Nephrol. 2019;20(1):268.

36 Hu PP, Bao JF, Li A. Roles for fibroblast growth factor-23 and α-Klotho in acute kidney injury. Metabolism. 2021;116:154435.

37 Zauderer MG, Szlosarek PW, Le Moulec S, Popat S, Taylor P, Planchard D, et al. Ezh2 inhibitor tazemetostat in patients with relapsed or refractory, bap1-inactivated malignant pleural mesothelioma: a multicentre, open-label, phase 2 study. Lancet Oncol. 2022;23(6):758–67.

38 Italiano A, Soria JC, Toulmonde M, Michot JM, Lucchesi C, Varga A, et al. Tazemetostat, an ezh2 inhibitor, in relapsed or refractory b-cell non-hodgkin lymphoma and advanced solid tumours: a first-in-human, open-label, phase 1 study. Lancet Oncol. 2018;19(5):649–59.

39 Morschhauser F, Tilly H, Chaidos A, McKay P, Phillips T, Assouline S, et al. Tazemetostat for patients with relapsed or refractory follicular lymphoma: an open-label, single-arm, multicentre, phase 2 trial. Lancet Oncol. 2020;21(11):1433–42.